Journal of Structural Geology, Vol. 7, No. 1, pp. 1 to 10, 1985
Printed in Great Britain

0191-8141/85 $03.00 + 0.00
Pergamon Press Ltd.

Footwall geometry and the rheology of thrust sheets

R. J. KNIPE

Department of Earth Sciences, University of Leeds, Leeds LS2 9JT, U.K.

(*Received* 19 *September* 1983; *accepted in revised form* 1 *August* 1984)

Abstract—The inter-relationships between the exact footwall geometry and the rheology of thrust sheets are investigated. Deviations in the thrust fault surface from an ideal plane will induce a local heterogeneous deformation. The resulting deformation processes depend upon the rate of thrust sheet displacement, the geometry of the feature causing heterogeneous flow, the deformation conditions and the lithologies involved. Two classes of features are particularly important in causing heterogeneous deformation in thrust sheets. The first features are small perturbations on bedding planes which may be inherited sedimentary structures or produced during layer-parallel shortening; the second class of features are ramps, where the thrust sheet climbs up the stratigraphic section. Displacement over these features causes repeated, cyclic straining in the hanging-wall during movement. The strain rates associated with deformation at perturbations, ramps of different geometries and different displacement rates are estimated and used to discuss the influence of footwall geometry on the structural evolution of a thrust sheet. Particular attention is given to the range of fault rocks and deformation microstructures preserved after movement over a footwall with a complex geometry. Perturbations are suggested to be important in the localization of ramps, either because they create 'sticking points' near the fault tip during propagation or because they induce eventual failure in the hanging-wall after the movement over a number of these features raises the accumulated damage to a critical level. Analysis of the influence of the exact geometry of ramps on deformation processes during displacement leads to two important conclusions. Firstly, the exact geometry of ramps (i.e. the maximum dip angle and the straining distance from a flat to this maximum angle) may be used to estimate a maximum displacement rate of the thrust sheet. Secondly, the listric geometry of ramps may be an equilibrium shape adjusted to the displacement rate and the rheology of the hanging-wall. Adjustments towards the final geometry may involve the generation of shortcuts on either hanging- or footwall which reduce the imposed deformation rate in the hanging-wall during displacement.

INTRODUCTION

RECENT analysis of the geometry of thrust sheets, both in the field and in laboratory modelling (Elliott 1976a, b, McClay & Price 1981, Williams 1982, Berger & Johnson 1982) has increased our understanding of the structural evolution of thrust sheets. Complex sequences of faulting can now be unravelled (Elliott & Johnson 1980, Boyer & Elliott 1982, Price 1981) and restored cross-sections used to estimate the shortening across thrust belts (Dahlstrom 1969, Hossack 1979). The patterns of strain recorded within thrust sheets have been used successfully to identify zones of differential movement (Coward & Kim 1981, Fischer & Coward 1982) and to establish the complex strain histories which can arise within thrust sheets during their displacement (Pfiffner 1981, Butler 1982, Sanderson 1982).

However, despite the advances in the understanding of the geometrical evolution of structures within thrust sheets there have been few attempts to assess the interactions between the exact geometry of the footwall, the displacement rate and the rheology of the thrust sheet. Two features in a footwall are particularly important to deformation mechanisms and processes occurring within an overlying thrust sheet, they are: (a) the precise geometry of the bedding surfaces when preferentially used as detachment planes and (b) the exact shapes of ramps where the thrust climbs stratigraphic level. This paper integrates information on the detailed geometry of the footwall with analysis of deformation mechanisms in an attempt to gain insight into: (1) the location of ramp development and (2) the type, width and range of fault rocks developed during thrusting. In addition, the paper introduces the possibility of using the detailed geometry of ramps to estimate a maximum displacement rate for thrust sheets.

PROPAGATION AND DISPLACEMENT PROBLEMS IN THRUST SHEETS

The propagation and displacement of a thrust sheet depends on (a) the mechanical behaviour of the material around the potential fault and (b) the ease of continued slip on the fault surface. Where thrusts propagate through bedded sequences the bedding surfaces are commonly used as fault planes (flats). If the potential fault plane is perfectly planar or propagates in an exceptionally weak horizon (e.g. salt or shale) no deformation of the hanging-wall may be needed. In such cases only the resistance to sliding or shearing on the planar fault zone needs be considered in the analyses of the fault movement (see Hubbert & Rubey 1959). However, if the fault plane deviates from a perfectly planar feature there has to be some form of heterogeneous or local deformation in order for displacement to occur. Where only thin weak horizons are present then deformation may still be induced in the hanging-wall if the thin, weak horizon is unable to absorb all the heterogeneous flow. Deviations of the footwall away from an ideal plane may take two forms: (1) initial perturbations on bedding planes (Fig. 1) or (2) ramps, where the hanging-wall has to deform in order to flow over the feature.

The presence of perturbations and ramps induces a local mechanical reaction which allows the fault to continue propagating or allows continued displacement. The nature of this reaction will depend on: (a) local environmental factors, such as the imposed displacement rate of the thrust sheet and its effect on the local stress levels, the temperature, the confining pressure, and the mechanical and chemical effects of any water present and (b) lithological controls such as the composition and microstructure of the rocks at the perturbation or the ramp. The possible reactions which may take place in the hanging-wall or footwall during movement over or propagation at a perturbation are reviewed in Fig. 2. If the reaction is in the footwall, then a fast imposed displacement rate leads to a fast local strain rate which will cause failure across a perturbation (Fig. 2a). In this case the perturbation may become part of the hanging-wall and be displaced along the fault. If the displacement rate, and thus the induced strain rate, is lower, then the perturbation may deform by dislocation processes, which may, with work hardening, eventually lead to failure (Fig. 2b). At even lower strain rates and in the presence of water the perturbation may migrate along the fault by diffusion mass transfer (see Elliott 1976, Rutter 1976, 1983) (Fig. 2c). Alternatively, if the reaction is in the hanging-wall a high displacement rate will induce failure and possibly the development of a ramp (Fig. 2d), while at slower displacement rates internal flow by dislocation processes or diffusive mass transfer will take place as the hanging-wall moves over the perturbation (Figs. 2e & f).

In the case of movement over a ramp the dependence of the flow behaviour on the displacement rate is identical. A fast displacement rate will induce failure in the hanging-wall and the development of a network of fractures, while a slower displacement rate will induce internal flow either by dislocation processes or by diffusion mass transfer processes.

The aim of this paper is to illustrate how semi-quantitative analysis of these various flow reactions is possible and to discuss the consequences of these reactions in terms of thrust-sheet displacement rate and rheology. The models presented are considered to be a first-order solution which can be improved as understanding of rock deformation processes increases. The paper is divided into two sections, the first presents a model for assessment of the reactions and strains associated with perturbations and ramps, while the second uses the geometry and sizes of the perturbations and ramps to assess the strain rates and deformation processes associated with these features.

DEFORMATION PROCESSES AT RAMPS AND PERTURBATIONS

The strain and stress patterns developed in a hanging-wall during displacement over a ramp have been modelled and discussed by numerous authors (e.g. Wiltschko 1979, 1981, Berger & Johnson 1980, 1982, Fischer & Coward 1982, Sanderson 1982). Sanderson (1982) presented two simple models of the straining process; one a 'bending' model involving vertical shear at the ramp and the other a 'flexural flow' model where beds retain their orthogonal thickness. In both cases the material entering the ramp suffers a shear strain which is reversed upon leaving the ramp and moving on to the upper flat. The shear strains induced in the hanging-wall at the ramp for various models are very similar and to analyse the deformation processes at both perturbation and ramps (half a perturbation) a kink-band like model has been selected here (Fig. 3). For the chosen model the shear strain predicted is given by

$$\gamma = \cot \alpha' - \cot \alpha, \qquad (1)$$

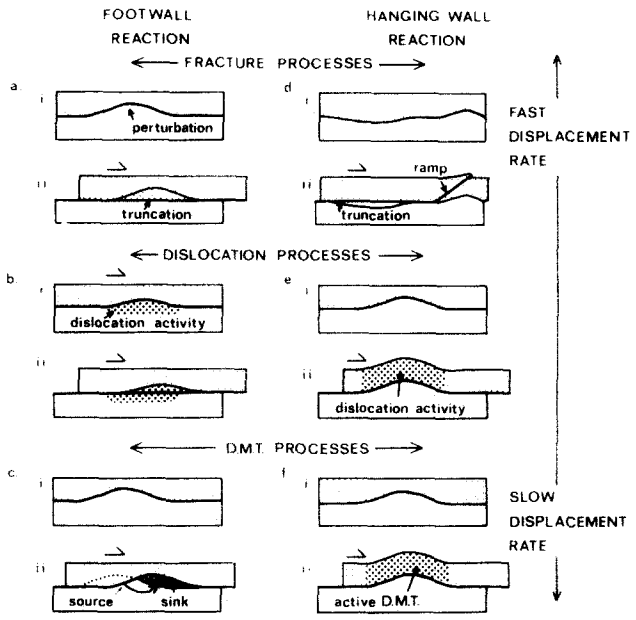

Fig. 2. Possible mechanical reactions at perturbations. The reaction may occur in either the hanging-wall or footwall. At fast displacement rates fracturing takes place, while at lower displacement rates internal ductile deformation, either by dislocation movement or diffusion mass transfer (DMT) takes place.

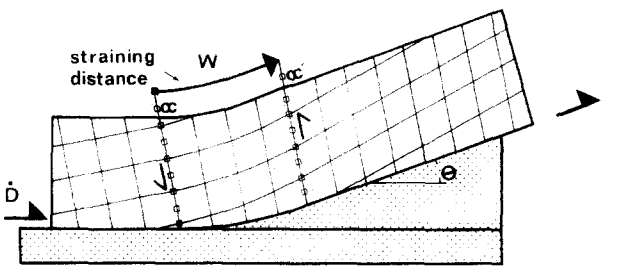

$$\gamma = 2 \tan \theta/2 . \qquad \dot{\gamma} = \frac{\gamma}{W/\dot{D}}$$

$$= \cot \alpha' - \cot \alpha .$$

Fig. 3. Straining model for deformation at a ramp (or part of a perturbation). The displacement rate, $\dot{D}$, induces a shear strain, γ, during movement through the straining distance, W. The straining can be considered to be progressive simple shear which alters the initial angle, α, of bedding to the shear plane to the final angle, α'. The strain rate, $\dot{\gamma}$, can thus be related to the displacement rate (D), the straining distance (W) and the dip of the ramp (θ).

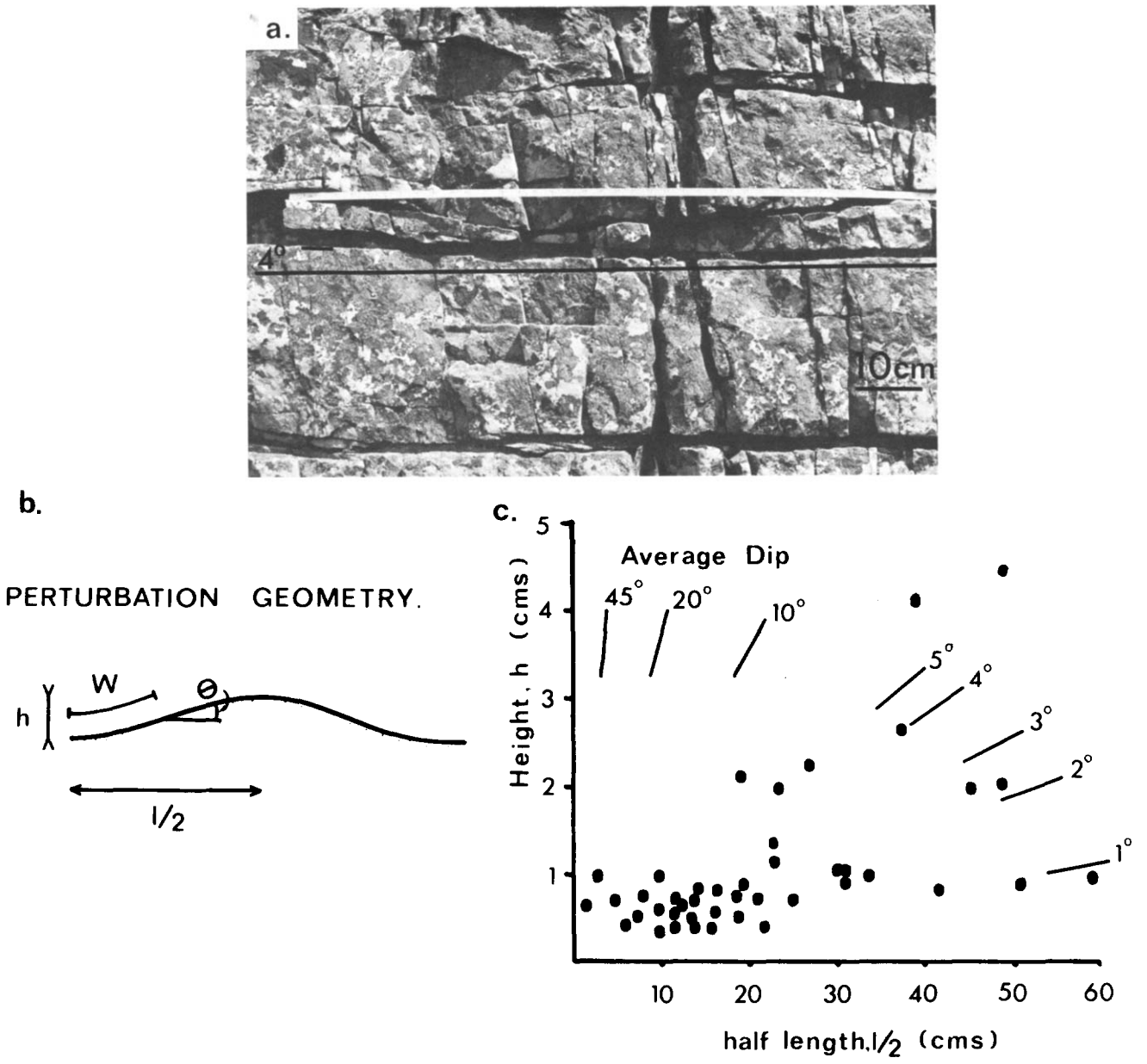

Fig. 1. (a) Bedding plane perturbations in the foreland region of the Moine Thrust zone at Assynt. The main bedding plane (centre) shows a 4° large-wavelength perturbation. Perturbations with smaller wavelengths are also present. (b) Elements of perturbation geometry important in the assessment of the effect of these features on thrust sheet rheology. h, perturbation height; l, length; θ, the maximum angle of dip; W, the straining distance measured from the flat to the maximum angle of dip. (c) Graph of the length, height and average dip of perturbations measured in the Eriboll Quartzite from the foreland area of the Moine Thrust zone at Loch Assynt. Perturbations with dips below 1° or lengths above 1 m were not measured.

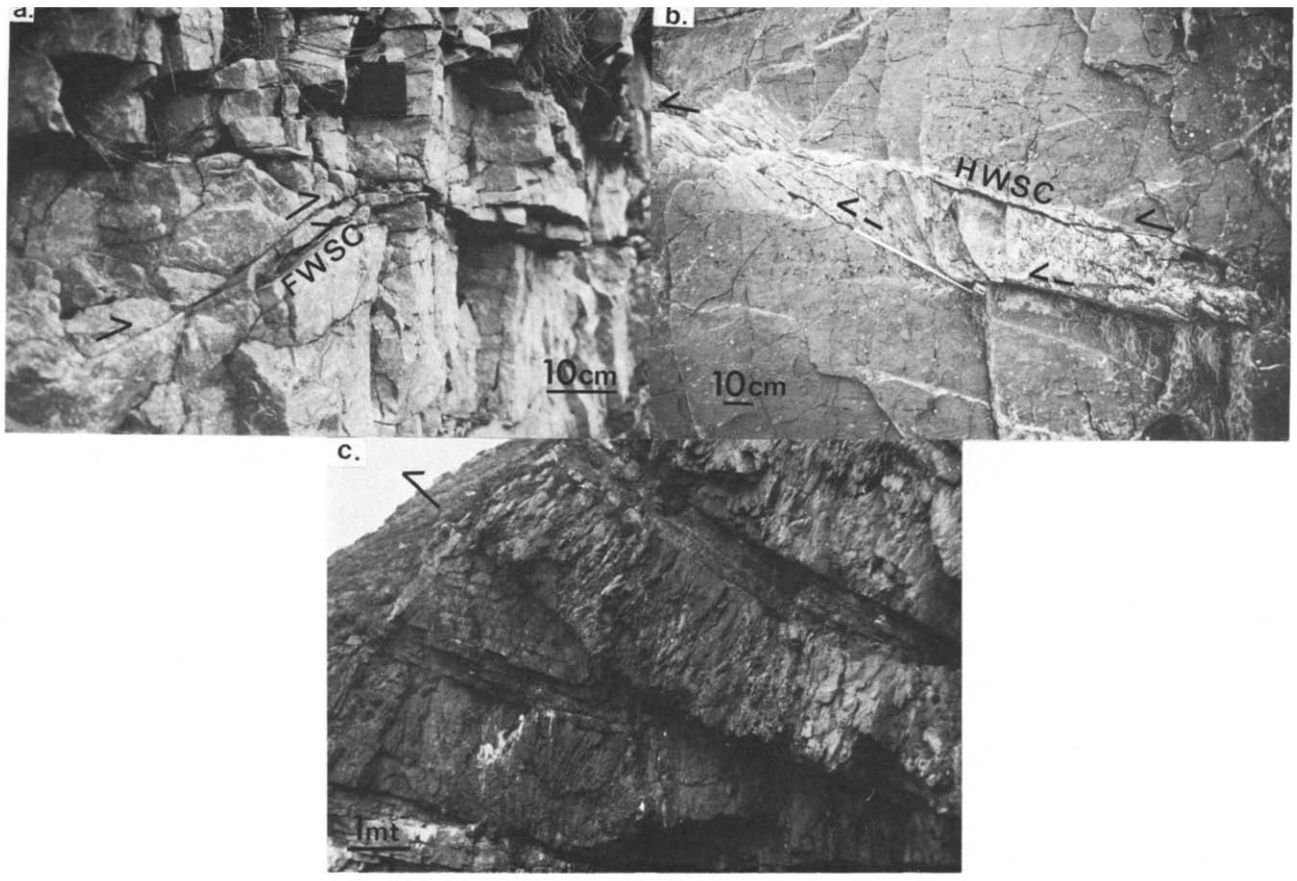

Fig. 12. (a) A footwall short cut (FWSC) developed in Cambrian Quartzite at Assynt, Scotland. (b) A hanging-wall short cut (HWSC) developed near a thrust tip in Carboniferous rocks at Tutt Head, the Mumbles, near Swansea. Note also the cleavage developed by shortening along the thrust. (c) Ramp developed in Cambrian Quartzite at Loch Eriboll (487 663) Scotland. The maximum dip of the ramp is 35° and the straining distance approximately 7 m.

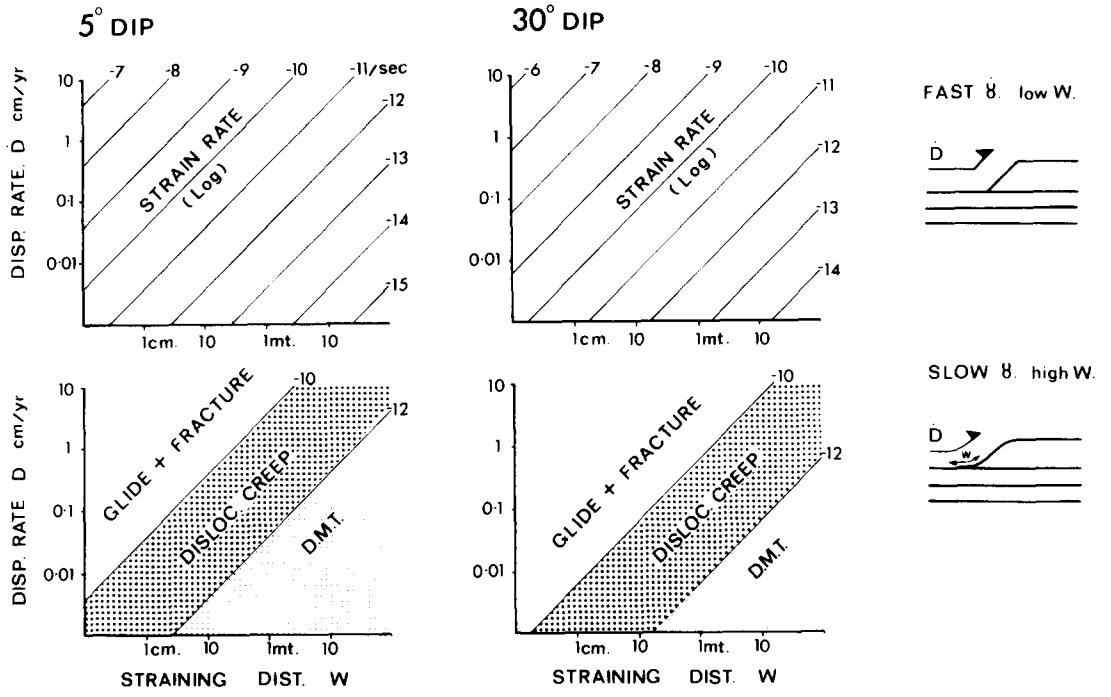

Fig. 4. Strain rates and deformation mechanisms associated with ramps or perturbations of different geometries. The top two graphs illustrate the strain rates, $\dot{\gamma}$, associated with differing displacement rates, $\dot{D}$; and straining distances, W for dips of 5 and 30°. The diagrams illustrate the reduction in strain rate associated with either increasing the straining distance, W, or decreasing the maximum angle of dip at a constant displacement rate. The lower diagrams illustrate the corresponding deformation mechanisms expected to dominate in a quartzite (grain size 0.1–0.5 mm), moving over perturbations or ramps at a temperature of 250–300°C. The distribution of deformation mechanism fields is based on the deformation mechanism maps of Rutter (1976) and White (1976). The conditions were chosen to model the deformation conditions experienced by the Eriboll Quartzites in the lower thrust sheets in the northern section of the Moine Thrust belt of Scotland. DMT, diffusion mass transfer.

where θ, is the dip of the ramp (from Fig. 3), α' and α are the final and initial angles between bedding and the axial planes of the induced folds. The axial planes of these folds can be considered parallel to the boundary of the shear zone which created the deformation (see Fig. 3).

The strain rate ($\dot{\gamma}$) induced in the hanging-wall as material moves (or attempts to move) over a perturbation or up a ramp will be a function of: (a) the imposed strain, which depends upon the dip (θ) of the perturbation or ramp and (b) the duration of the strain accumulation, which depends on both the imposed displacement rate ($\dot{D}$) and the displacement distance (W) over which strain accommodation occurs (see Fig. 3),

$$\dot{\gamma} = \frac{\gamma}{(W/\dot{D})}. \quad (2)$$

Given a fixed maximum dip value a short straining distance (i.e. a small radius of curvature) or a fast displacement rate will induce a fast strain rate in the hanging-wall. Using a selected range of displacement rates and straining distances it is now possible to calculate the strain rates induced in the hanging-wall during flow over perturbations or ramps with different geometries. These are presented in Fig. 4, which also illustrates the deformation mechanism which would be dominant in a quartzite at approximately 250°C (see caption for details). The diagrams show that for a displacement rate of 1 mm a^{-1} and a dip of 30° the strain rate varies from 10^{-10} s^{-1} to 10^{-12} s^{-1} if the straining distance (W) varies from about 10 cm to 10 m. For the Pipe Rock Quartzite at Assynt in the Moine Thrust zone (see McClay & Coward 1981 for a regional review) where the temperature of deformation is considered to have been 200–250°C, the range of geometries recorded for perturbations (Fig. 1) indicates that deformation mechanisms involving dislocation movement would be prevalent in the hanging-wall if the displacement rate was above 0.1 mm a^{-1}.

In order to assess which strain rates are high enough to induce fracture of the material as it passes over a perturbation, or up a ramp, information on the relationship between strain rate and strain to failure is required. At high strain rates failure is preceded by small elastic strains (≤3%). At lower strain rates failure by ductile fracturing may eventually arise, after high strains, from two situations. (1) The material builds up a high internal damage and strain energy; that is when the work hardening rate exceeds the recovery rate. This will occur when, for example, dislocation pile ups are created faster than dislocation annihilation and recovery into low energy configurations can take place (White 1976). (2) The second process which may lead to failure at low strain rates is the linking of creep voids created at grain boundaries. Thus the microstructural processes responsible for failure or fracture will vary with different strain rates. The strain rate marking the transition between different fracture models and the strain rate below which large ductile strains (>10) can be achieved will be strongly

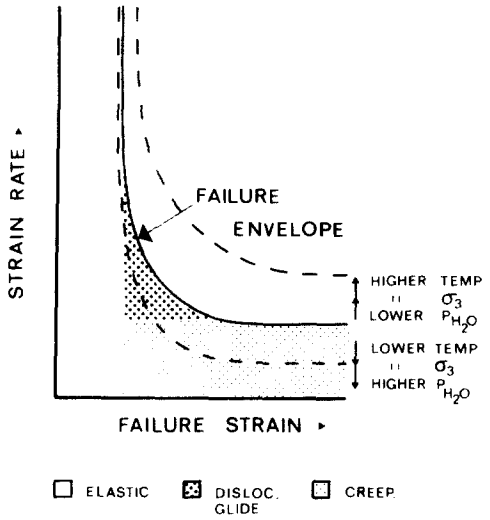

Fig. 5. The effect of strain rate, temperature, confining pressure (σ_3) and pore water pressure (P_{H_2O}) on the strain to failure.

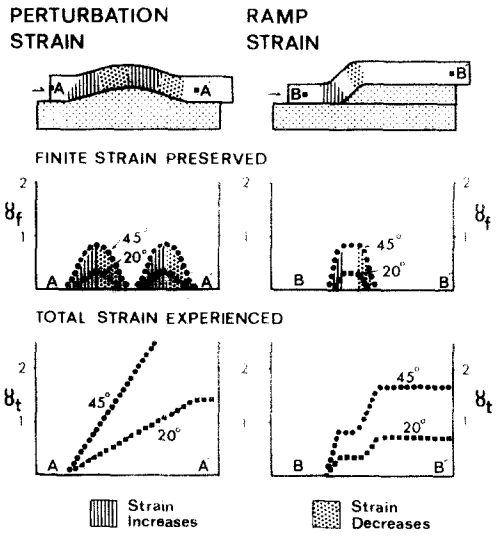

Fig. 6. Comparison of the finite strain preserved, γ_f, and the total strain experienced, γ_t, during movement over perturbations and ramps. Note the alternating cycles of increasing and decreasing finite strain and the ever increasing total strain experienced. For details see text.

dependent upon the temperature, confining pressure and pore fluid pressure (Fig. 5). The critical strain rate below which large ductile strains are possible may be associated with the transition from conditions where the production of internal damage is faster than recovery processes. The transition is expected to occur at the change over between deformation dominated by dislocation glide (where tangles and pile-ups lead to work hardening and failure) and dislocation creep (where recovery and recrystallization processes allow continued deformation). The published deformation mechanism maps for quartz (Rutter 1976, White 1976) indicate that this transition takes place at strain rates of approximately 10^{-10} s^{-1} to 10^{-11} s^{-1} for a temperature of 250–300°C and a grain size of 0.1 mm. Thus in order to prevent work hardening and failure in the Eriboll Quartzite (grain size 0.1–0.5 mm) at this temperature a strain rate below 10^{-10} s^{-1} will be needed. This estimate can be used to speculate on which perturbations or ramp geometries allow continued flow in the hanging-wall without fracturing. For example, to prevent failure at a perturbation or ramp with a maximum dip of 30° the displacement rates would have to be below 0.5 mm a^{-1} and 5 mm a^{-1} if the straining distances were 10 cm or 1 m, respectively. Alternatively, if the displacement rate is fixed at 1 mm a^{-1} then, in order to prevent failure, a perturbation or ramp with a 5° dip has to have a straining distance greater or equal to 3 cm, while a perturbation or ramp with a dip of 30° requires a straining distance of at least 10 cm.

CYCLIC OR REPEATED STRAINING WITHIN THRUST SHEETS

Figure 6 illustrates the variation in the shear strain induced in the hanging-wall as material moves over a perturbation and a ramp. The diagram emphasizes the cyclic changes which can occur in the finite strain states and compares them with the progressive increase in the total strain experienced by the material. Thus while the finite strain oscillates up and down, the total strain experienced increases; that is, the material may be accumulating internal damage.

Even if the strain rate associated with movement over a single perturbation or ramp can be accommodated without failure, continued movement over additional features may lead to eventual failure. This situation is illustrated in Fig. 7, where the material accumulates strain in a ductile fashion up to a certain level before failure takes place. Failure in this case is associated with a build up in the internal strain energy or cumulative damage within the material. At high strain rates this can result from the linking of micro-cracks before large-scale failure takes place, while at lower strain rates it may be associated with dislocation interactions inducing work-hardening before failure.

Unfortunately this deformation situation, of cyclic straining episodes separated by rest periods, has hardly been investigated in experimental rock deformation. In the case of metals this deformation behaviour has been studied extensively and is termed fatigue (see Barnby 1972, Frost *et al.* 1974). The variables which are important to the behaviour of material undergoing this type of

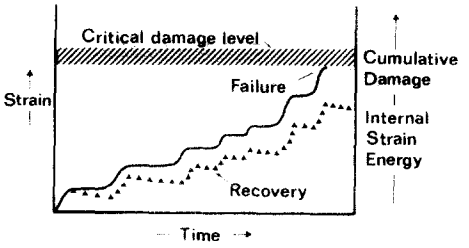

Fig. 7. Changes in strain accumulation with time. Increases in strain, associated with flow over perturbations, or ramps, are separated by non-accumulation 'rest' periods. Increases in the cumulative damage or internal strain energy to some critical level induces failure. However, recovery between straining events reduces the internal strain energy and postpones failure.

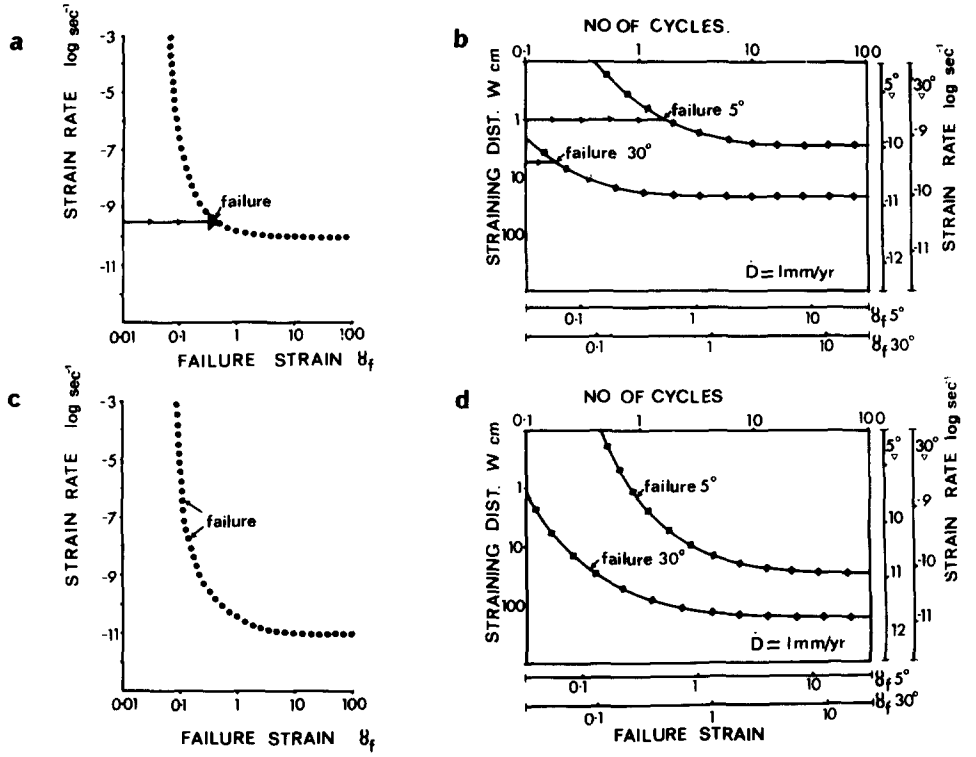

Fig. 8. Estimation of the number of pre-failure strain cycles for a quartzite. (a) Possible interrelationship between strain rate and failure strain for a quartzite at 250–300°C. The lower limit of strain rates which lead to failure is estimated from the change over of deformation dominated by dislocation glide and deformation dominated by dislocation creep (see text for details). The strain failure at high strain rates is estimated from Handin (1966). (b) Relationship between strain rate; total strain before failure (γ_f) straining distances (W) and the number of strain cycles before failure for perturbations or ramps with dips of 5 or 30°, where the displacement rate is 1 mm a^{-1}. The diagram serves to illustrate which ramp or perturbation geometries allow continued ductile deformation and those which eventually lead to failure. (c) and (d) Situation for failure strain rate of 10^{-11} s^{-1}.

deformation are: (1) the range of stress levels, both differential and mean, and their rate of variation during each cycle; (2) the strain path for each cycle; (3) temperature and (4) the duration of the stress cycle and the duration of the (rest) period between straining. Each of these variables is important in assessing the behaviour of material within thrust sheets where strain cycles are associated with movement over perturbations and ramps. If recovery of cumulative damage (e.g. recrystallization, annealing) is possible during these rest periods then a larger displacement may take place prior to failure (Fig. 7). Such recovery is favoured by high temperatures (faster recovery) and slow displacement rates (longer rest periods between straining events).

In the absence of experimental data on the strain which can accumulate in rocks by cyclic deformation before failure, it is impossible at present to estimate accurately the number of cycles (i.e. the number of perturbations or ramps encountered) before failure occurs. However it is possible to use a speculative example to illustrate the potential effect of different perturbation angles and straining distances on the number of cycles (i.e. number of perturbations or twice as many ramps) encountered before failure. Figure 8 illustrates the results of such an estimate for quartzites at 250°C where the displacement is fixed at 1 mm a^{-1}. The diagram serves only to illustrate a general deformation behaviour, the quantification of which awaits experimental results on the slow cyclic deformation of rocks.

DISCUSSION

The models presented above illustrate a method of assessing the deformation processes and straining conditions at perturbations and ramps. The calculations serve only as an indication of the rates of deformation but do allow an insight into the processes that can induce failure in a thrust sheet. This section uses field data on the detailed geometry of ramps and perturbations to investigate the application of the models presented to the evolution of a thrust sheet. Particular attention is given to the following aspects of thrusting: (a) thrust fault location, (b) evolution of deformation microstructures and fault rocks, (c) location and listric geometry of ramps and (d) estimation of the maximum displacement rate of the thrust sheet.

Thrust fault locations

The analysis presented indicates that in a bedded sequence a thrust fault will be nucleated or propagate on bedding planes which have the least number and/or the lowest amplitudes, and/or the longest wavelengths of perturbations. The effect of different perturbation geometries on the strain rate induced in the hanging-wall is best illustrated by an example. Figure 9 shows the effects of the exact geometry of three adjacent bedding planes, located within the Lower Cambrian Quartzite adjacent to the Moine Thrust belt of Assynt, NW Scot-

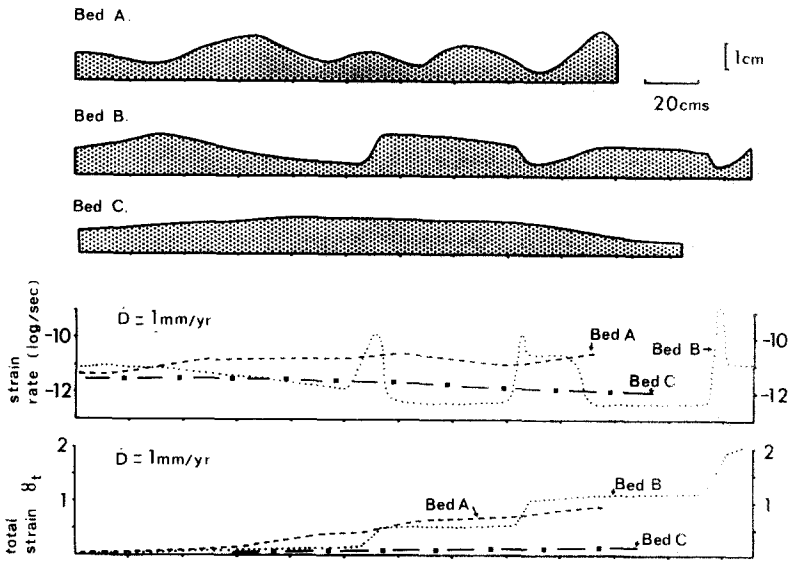

Fig. 9. Variation in the strain rate and total strain experienced with displacement over three bedding planes (A, B and C), based on measurements of exact geometry of these bedding planes. These bedding planes are from within the Cambrian Quartzite of Assynt and are located just outside the thrust belt. The strain rates were calculated from equation (2). The diagrams serve to show; (i) the range of strain rates induced by constant displacement rate over perturbations with varying geometry and (ii) the build up of total strain experienced which eventually can induce failure. Note that although Bed A geometry produced a higher average strain rate, Bed B geometry induces a higher total strain. This arises because perturbations on Bed B have higher angles and are longer than perturbations on Bed A. This illustrates the two causes of failure which may be induced in a hanging-wall, one by exceeding a critical strain rate and the other by exceeding a critical internal strain energy associated with the total strain experienced.

land. No shale units are present along these bedding planes. Of the three bedding planes shown, Bed C is the most planar and therefore offers the least resistance to slip.

Evolution of deformation microstructures and fault rocks

In the case of a high displacement rate which induces truncation of the perturbations the zone of brecciation along the fault, which results, should have a width approximately equal to the height of the perturbations. It is interesting that where thrust breccia zones are present in the Cambrian quartzites of the Moine Thrust belt their width is commonly less than 5 cm; that is approximately equal to the maximum height of perturbations on bedding planes in the foreland (see Fig. 1).

The selected bedding planes shown in Fig. 9 also serve to illustrate the effect of perturbation geometry and size on the strain rate, strain accumulation and microstructural evolution during deformation in the hanging-wall when the displacement rate is held constant. Bedding plane B shows that the strain rate induced during displacement may vary over three orders of magnitude for material near the fault plane. This range of induced strain rates is fundamental to the microstructural development of rocks during thrusting. Any small unit of rock near the fault plane will develop a wide range of microstructural features (each associated with different strain rates) which will be superimposed upon each other in a complex fashion dependent upon the variable geometries of the perturbations and ramps it passes over. For this reason the microstructures present in the vicinity of thrust faults are not good indicators of 'average' conditions of processes of deformation taking place in the thrust sheet during displacement, but indicate the local heterogeneous processes at the fault. For example propagation of the fault along a bedding plane with a large number of steep or short perturbations may lead to the development of a discontinuous zone of brecciation. Specimens collected away from this 'contact strain zone' will be more useful for the assessment of deformation processes at ramps.

Location and listric geometry of ramps

The analysis presented above suggests that perturbations may influence the location of ramp development in two ways. The first is when a perturbation restricts propagation, that is, causes 'sticking' of the fault tip. In this case a ramp may develop during the first attempt to flow over a perturbation. If the displacement rate is high then the induced strain rate may be great enough to initiate failure and ramp development. If the displacement rate is lower, or the propagation rate of the fault slow, then layer-parallel shortening and eventually folding may take place at the tip of a propagating thrust held up at the perturbation. This is essentially the situation analysed by Berger & Johnson (1980, 1982). In this case the layer-parallel shortening in the hanging-wall propagated back along the fault from the fault tip and the eventual failure of the fold to produce a ramp can be considered one end member reaction to overcome the flow heterogeneity introduced by the perturbation (Fig. 10).

The second way in which perturbations may influence ramp development is when cumulative damage induced

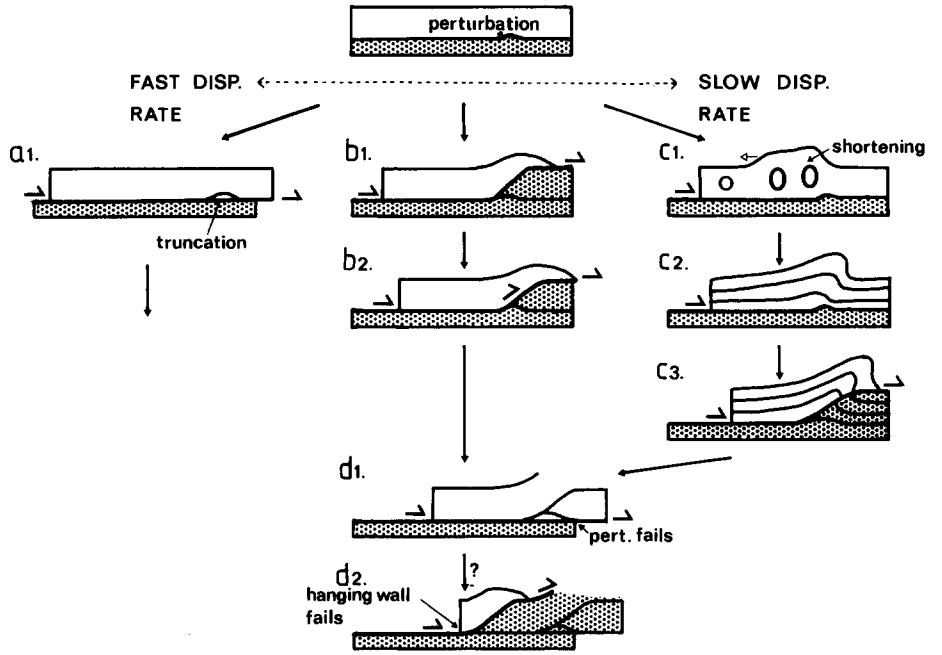

Fig. 10. Idealized deformation history and structures produced by different mechanical reactions induced by sticking at a perturbation during different displacement rates. Fast displacement rates decapitated perturbations (a_1), while slower displacement rates can induce ramp formation after small amounts of hanging-wall strains (b_1, b_2). At even slower displacement rates layer-parallel shortening strains may spread back from the tip (c_1, c_2) and folding predate ramp development (c_2–c_3). Footwall collapse and the generation of a new thrust fault into the foreland may be associated with strain damage accumulation in the perturbation, reaching a critical level (d_1). Finally movement over low angle or large wavelength perturbations may induce a similar failure in the hanging-wall and the generation of an out of sequence thrust (d_2).

by flow over a number of perturbations results in failure. This situation is a possible cause of the initiation of an out-of-sequence thrust (see Fig. 10). In both the production of ramps at, and away from tips, it is suggested that the interaction of the stress field around the perturbation and the larger scale stress pattern within the thrust sheet controls the orientation of the ramp, which in some cases may be a lateral ramp or a strike-slip fault.

The estimates of strain rate from ramp geometry discussed above (Fig. 4) can also provide an insight into the evolution of the listric shape of ramps. A perturbation may lead to a hanging-wall failure and production of a ramp fault which is initially too steep or too angular for flow to occur up the ramp without failure (Fig. 11a). As an alternative to large-scale fracturing of the hanging-wall, a single fracture may form in the zones of high curvature (Fig. 11b). These form either hanging-wall short cuts or footwall short cuts which increase the straining distances and reduce the strain rate needed in the hanging-wall during displacement over the ramp. Repeated adjustments like this will lead to a listric geometry. That is, the listric geometry can be regarded

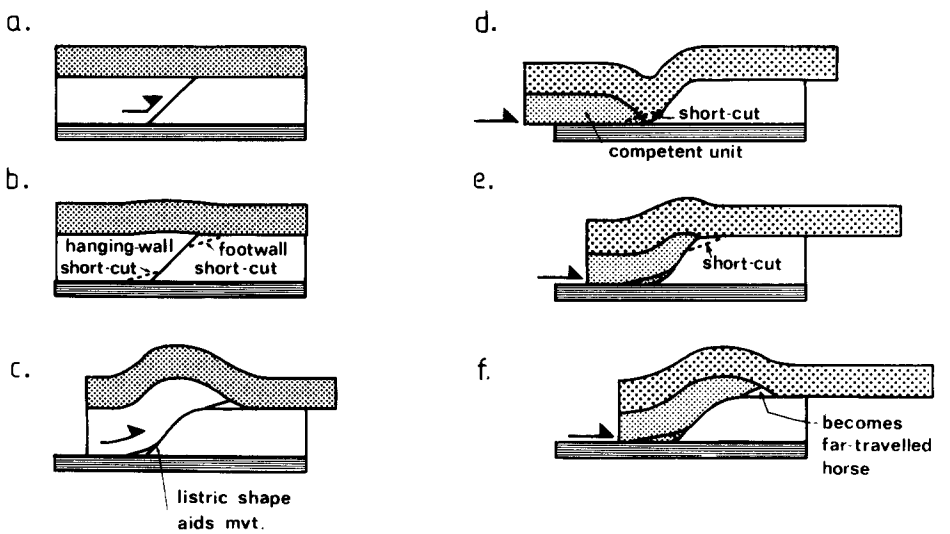

Fig. 11. Adjustments to ramp geometries to aid movement of hanging-wall. Sequence (a)–(c) illustrates the generation of hanging-wall short-cuts and footwall short-cuts which increase the straining distance and produce a listing ramp geometry. Sequence (d)–(f) illustrates the changes in ramp geometry which may be induced by a competent unit attempting to climb a ramp. The arrival of such a competent unit at the base of a ramp may also induce footwall collapse by resisting bedding.

as a low-energy equilibrium feature adjusted to minimize the strain rate in the hanging-wall during displacement. Possible examples of short-cut process are illustrated in Figs. 12(a) & (b). Such adjustments to the ramp geometry may also be produced when changes in the displacement rate occur or beds of different lithologies and therefore different rheologies move over a ramp (Figs. 11d–f). One consequence of the above process is the production of triangular fault-bounded 'horses' where footwall shortcuts develop. These horses are accreted to the hanging-wall and may become the 'far travelled horses' seen in some thrust belts.

Estimation of maximum displacement rates in thrust sheets

By combining information on the exact geometry of ramps measured in the field and analysis of the deformation mode in the hanging-wall with the graphs of strain rate versus straining distances for different ramp dips (Fig. 4), it is possible to estimate the maximum displacement rate of the thrust at this point if the strain rate which caused failure is known. An example is shown in Fig. 12(c) where the ramp has a dip of 30° and a straining distance of 7 m. In order to prevent failure (i.e. to keep the strain rate below $10^{-10}\,s^{-1}$) the displacement rate has to be below 4 cm a^{-1}. The estimate is interesting in that it accords with values of displacement rates determined for thrust sheets based on stratigraphical and sedimentological data (see Elliott 1976).

CONCLUSIONS

The analysis presented above illustrates how the exact geometry of the footwall to a thrust sheet can influence the deformation and rheology within the sheet. The following important points emerge from the analysis.

(1) Steep or short perturbations in the footwall can induce local sticking and high strain rates which themselves promote a ramp development at the thrust tip zone during the early stages of displacement. The exact ramp evolution process can be related to the displacement rate, the confining pressure and the strength of the material. High displacement rates and low confining pressures (and high P_{H_2O}) induce fracture after very low strains at the tip, while low displacement rates and high confining pressures (and low P_{H_2O}) promote folding before ramp development.

(2) Local modifications may be needed at ramps, for example shortcuts, to allow flow over ramps. Such shortcuts result in the development of listric fault geometries.

(3) Gentle or long perturbations together with ramps in the footwall cause cyclic deformation which may lead to the build up of cumulative strains in the hanging-wall which can result in the production of a ramp behind the thrust tip zone. If the failure is a long way behind the tip zone an out-of-sequence thrust may develop.

(4) Cyclic-straining is associated with movement over perturbations and ramps, and will create a wide range of different deformation microstructures superimposed upon each other as rocks move over perturbations and ramps of different geometries.

(5) The exact geometry of ramps (that is the maximum angle of dip and straining distance) can be used to estimate maximum displacement rates in thrust sheets.

Acknowledgements—I thank my colleagues, especially Mike Coward, Ernie Rutter, Graham Potts, Robert Butler and Dave Elliott for discussions and comments on an initial draft. The paper was initially presented at a Tectonic Studies Group Meeting on The Brittle Ductile Transition in Rocks held at Birmingham in November 1982. The research was supported by N.E.R.C. Grants GR3/4100 and GR3/4612.

REFERENCES

Barnby, J. T. 1972. *Fatigue*. Mills & Boon, London.
Berger, P. & Johnson, A. M. 1980. First-order analysis of deformation of a thrust sheet moving over a ramp. *Tectonophysics* **70**, T9–T24.
Berger, P. & Johnson, A. M. 1982. Folding of passive layers and forms of minor structures near termination of blind thrust faults—Application to the Central Appalachian blind thrust. *J. Struct. Geol.* **4**, 343–353.
Boyer, S. E. & Elliott, D. 1982. Thrust systems. *Bull. Am. Ass. Petrol. Geol.* **66**, 1196–1230.
Butler, R. W. H. 1982. Hanging wall strain: a function of duplex shape and footwall topography. *Tectonophysics* **88**, 235–246.
Coward, M. P. & Kim, J. H. 1981. Strain within thrust sheets. In: *Thrust and Nappe Tectonics* (edited by McClay, K. R. & Price, N. J.). *Spec. Publs geol. Soc. Lond.* **9**, 275–292.
Dahlstrom, C. D. A. 1969. Balanced cross sections. *Can. J. Earth Sci.* **6**, 743–746.
Elliott, D. 1976. The energy balance of thrust sheets. *Phil. Trans. R. Soc.* **A283**, 289–312.
Elliott, D. & Johnson, M. R. W. 1980. Structural evolution of the northern part of the Moine Thrust zone. *Trans. R. Soc. Edinb., Earth Sci.* **71**, 69–96.
Fischer, M. W. & Coward, M. P. 1982. Strains and folds within thrust sheets: an analysis of the Heilam sheet, northwest Scotland. *Tectonophysics* **88**, 291–313.
Frost, N. E., Marsh, K. J. & Pook, L. P. 1974. *Metal Fatigue*. Clarendon Press, Oxford.
Handin, J. 1966. Strength and ductility. In: *Handbook of Physical Constants* (edited by Clark, S. P.). *Mem. geol. Soc. Am.* **97**, 223–291.
Hossack, J. R. 1979. The use of balanced cross-sections in the calculation of orogenic contraction—a review. *J. geol. Soc. Lond.* **136**, 705–711.
Hubert, M. K. & Rubey, W. W. 1959. Role of fluid pressure in mechanics of overthrust faulting. *Bull. geol. Soc. Am.* **70**, 115–166.
McClay, K. R. & Price, N. J. (Eds). 1981. *Thrust and Nappe Tectonics. Spec. Publs geol. Soc. Lond.* **9**, 1–539.
Pfiffner, O. A. 1981. Fold and thrust tectonics in the Helvetic Nappes, Switzerland. In: *Thrust and Nappe Tectonics* (edited by McClay, K. R. & Price, N. J.). *Spec. Publs geol. Soc. Lond.* **9**, 319–329.
Price, R. A. 1981. The Cordilleran foreland thrust and fold belt in southern Canadian Rocky Mountains. In: *Thrust and Nappe Tectonics* (edited by McClay, K. R. & Price, N. J.). *Spec. Publs geol. Soc. Lond.* **9**, 426–448.
Rutter, E. H. 1976. The kinetics of rock deformation by pressure solution. *Phil. Trans. R. Soc.* **A283**, 203–219.
Rutter, E. H. 1983. Pressure solution in nature, theory and experiment. *J. geol. Soc. Lond.* **140**, 725–740.
Sanderson, D. J. 1982. Models of strain variation in nappes and thrust sheets: a review. *Tectonophysics* **88**, 201–235.
White, S. H. 1976. The effects of strain on the microstructures, fabrics and deformation mechanisms of quartzite. *Phil. Trans. R. Soc.* **A283**, 69–86.
Williams, G. D. (Ed.) 1982. *Strain within Thrust Belts. Tectonophysics* **88**, 201–362.
Wiltschko, D. V. 1979. Mechanical model for thrust sheet deformation at a ramp. *J. geophys. Res.* **84**, 1091–2204.
Wiltschko, D. V. 1981. Thrust sheet deformation. In: *Thrust and Nappe Tectonics* (edited by McClay, K. R. & Price, N. J.). *Spec. Publs geol. Soc. Lond.* **9**, 55–63.